Invited Paper

Infrared microantennas

Glenn D. Boreman

University of Central Florida
Department of Electrical Engineering
Center for Research & Education in Optics & Lasers (CREOL)
P. O. Box 162700
Orlando FL 32816-2700 USA

BOREMAN@CREOL.UCF.EDU

ABSTRACT

We present results of measurements of the polarization response of asymmetric spiral antennas coupled to Ni-NiO-Ni diodes, over the wavelength range 10.2 to 10.7 μm. The feed structure of the antenna imposes an elliptical polarization signature that is different from the circular polarization expected from a symmetric spiral. We develop a lossy-transmission-line model yielding the measured polarization response. A combination of a balanced and an unbalanced mode is required. Reflected current waves from the arm ends are significant.

Keywords: infrared detector, antenna

1. INTRODUCTION

In the design of very fast infrared detectors, the dimensions of the sensor element itself are often required to be smaller than the wavelength of the radiation to be detected. This is analogous to the usual situation with microwave and radiowave systems, where an antenna is to couple the oscillating radiation field into a sub-wavelength-sized sensor. Antennas of various configurations (dipoles, spirals, etc.) have been demonstrated[1-5] at wavelengths as short as 10 μm.

We have studied two different kinds of antenna-coupled sensors: bolometers and metal-oxide-metal (MOM) tunnel diodes. Both operate at room temperature, and have been demonstrated to receive radiation at a wavelength of 10 μm.

A typical antenna-coupled IR bolometer[1] has the following constructional characteristics: Si substrate with a few μm of SiO_2 overcoat (for thermal isolation), bolometer is a 200-Å-thick film of Niobium, few μm on a side, both arms of the antenna are deposited together on top of the bolometer in the same lithographic step. The Nb island is the resistance between the arms at the feed. The mechanism of operation is that the incident radiation excites IR-frequency current waves in antenna arms, which then propagate to the feed and are dissipated in the bolometer. The bolometer temperature increases causing a resistance change. Typical response time is on the order of a few milliseconds.

Typical antenna-coupled metal-oxide-metal (MOM)[2-5] diodes have the following constructional characteristics: Si substrate with a few μm of SiO_2 overcoat (for electrical insulation), diode dimensions: 0.2-μm-thick layer of Ni, 30-Å-thick layer of NiO, and another 0.2-μm-thick layer of Ni. The metal-oxide-metal (MOM) contact area is about 0.25 μm by 0.25 μm. Fabrication of this sensor requires oxide-layer growth between two successive lithographic steps (one for each arm) to make the layered MOM contact. The mechanism of operation is that the incident radiation exictes IR-frequency current waves in antenna arms which propagate to the feed. These currents produce an IR-frequency voltage across diode. The diode has a nonlinear current-voltage characteristic because of field-enhanced electron tunneling. The IR-frequency voltage is rectified, causing a dc resistance change. Typical response time is as short as a few picoseconds. The bolometric sensor is simpler to fabricate, but the MOM diode is much faster, facilitating applications in ultrafast spectroscopy.

2. CONFIGURATION EXAMPLE FOR IR ANTENNAS

To understand the conceptual operation of IR antennas, we consider the example of the half-wave dipole seen in Fig. 1.

SPIE Vol. 3110 • 0277-786X/97/$10.00

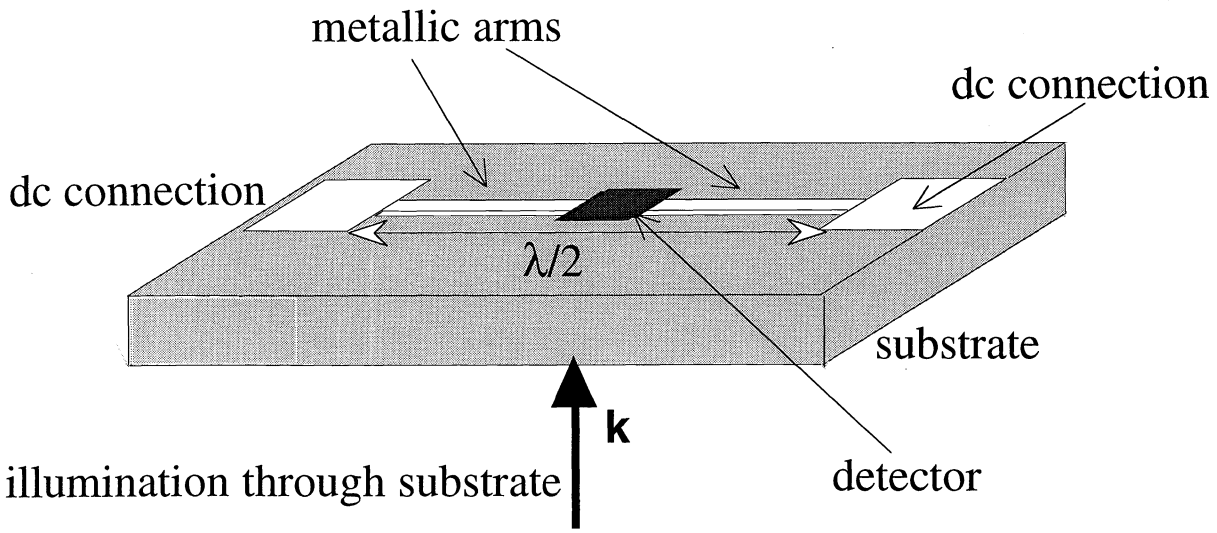

Fig. 1. Half-wave infrared dipole antenna.

IR antennas are typically illuminated through the substrate, since the reception is stronger[6] by a factor of $\varepsilon_r^{3/2}$ (a factor of 40 in Si). The incoming EM wave excites current waves in the arms of the antenna so that the radiation is coupled into the detector. For both bolometers and MOM diodes, incident radiation changes the dc resistance, which is measured by an external bridge circuit through the dc electrical leads. The detector element is small (compared to wavelength), so it would have a negligible radiation-capture cross section without an antenna.

3. SPECIFIC IR ANTENNA INVESTIGATED

We made polarization measurements[5] on a particular configuration of antenna, a MOM diode coupled to an asymmetric spiral. The feed structure has a 90° intersection which eases positioning tolerance between the two successive lithographic steps that are required to make the diode contact. The spiral-arm configuration of the antenna widens the wavelength response compared to the resonance bandwidth of a half-wave dipole. Because of the feed asymmetry, we expect that the polarization response for this antenna will be elliptical rather than circular.

4. TRANSMISSION-LINE MODEL FOR ANTENNA POLARIZATION

Travelling-wave current elements were assumed to travel tangent to the inside edge of the spiral structure (numerical modeling indicated that the inside edges have highest field strength). We thus used a a wire model coinciding with the inside edges of the arms. The current waves were assumed to have a wavelength equal to the substrate wavelength of the illuminating radiation inside the substrate (free space wavelength divided by substrate refractive index). The boundary conditions at the ends of the arms (π phase shift, total reflection) produce reflected current waves that propagate back toward the feed. The current-wave attenuation coefficient was measured[3] to be 0.15 μm^{-1} on similar IR dipole antennas, so this value was used in the model. With a one-way wire length $\approx$ 8 μm, secondary reflected waves are taken to be negligible. We considered the travelling current wave on each arm to propagate outward from the feed, for convenience in normalization. By the reciprocity theorem, this is equivalent to the measured case of the receiving antenna.

Every incremental vector current element is taken as a 30-THz dipole on a dielectric substrate.[7] For each current element on both wires we considered magnitude, direction, and accumulated phase from the feed point. The vector resultant of these incremental, closely-spaced dipoles at any instant in time will produce the instantaneous polarization vector. The orientation and magnitude of this vector change with time, tracing out the polarization ellipse during one period of the 30 THz oscillation.

The predicted polarization signature of a first-order calculation was used as a check on the model.

We assumed that the strongest current waves were at the (90°-intersection) feed region. Initially, we considered only the balanced mode (arms are π out of phase at the origin), and neglected the other (spiral) parts of the antenna and the reflected waves. Both arms supported outward-propagating waves, but with a π phase shift between arms, the instantaneous vector current elements are pointed toward the feed on one arm, and away from the feed in the other arm, as seen in Fig. 2.

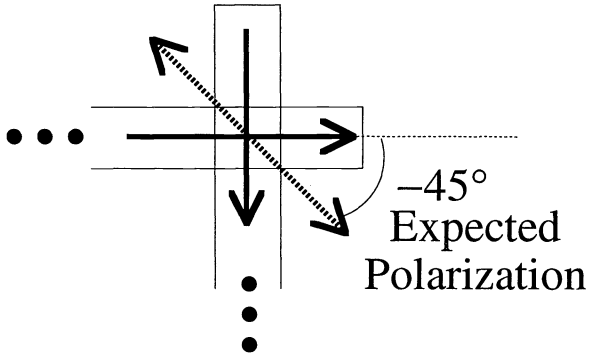

Fig. 2. Expected first-order polarization signature.

The major axis of the polarization ellipse (for the feed signature) was at $\theta = -45°$. The predicted orientation of the major axis did not change quadrant when the vector contributions from the rest of the spiral and the end-of-arm reflections were added. Measurements did not agree with this first-order prediction. We measured (at a wavelength of 10.7 μm) a major axis of the polarization ellipse at 30.8°, as seen in Fig. 3.

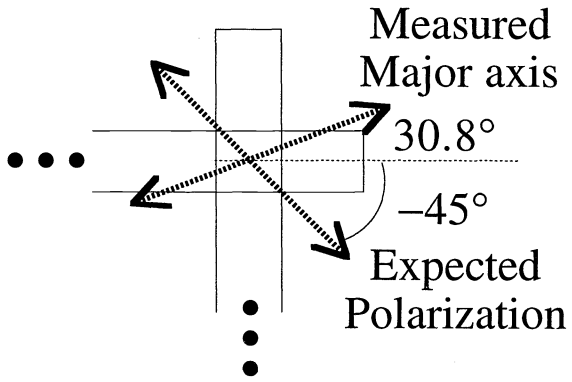

Fig. 3. Measured polarization signature at 10.7 μm.

From the discrepancy between the first-order model and the measurements, it was apparent that a more sophisticated model was needed. We then allowed two current-wave modes to propagate on the antenna: a balanced (phase shift π between arms) and an unbalanced (phase shift 0 between arms) mode as seen in Fig. 4. The mode-mixture ratio "U/B" was taken as a fitting parameter.

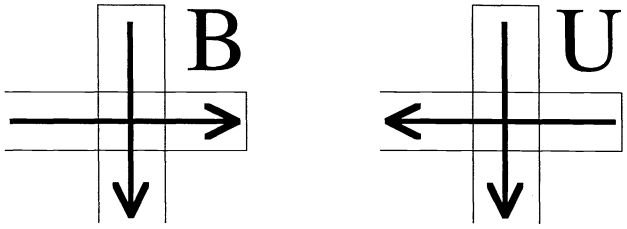

Fig. 4. Definition of balanced and unbalanced modes at the antenna feed.

We found that, although a U/B ratio could be found that produced the measured polarization angle, the proper value of this ratio depended critically on the length of the arms before reflection "L." We used a simple lumped-reflection model where the outgoing current wave will (on each arm) reverse its direction with unit reflectivity and π phase shift at a propagation distance L from the feed.

However, there is not truly an abrupt end to the arms, from an electrical point of view, but rather a distributed reflection. There are a number of factors influencing the exact value of L: arm curvature, unbalanced readout configuration, impedance of the arm termination. The value of L determines the phase relationship of the reflected waves at the feed point with respect to the outgoing waves, and hence affects the direction of the vector resultant. More measurements were needed to develop insight into the modes of the antenna structure, and to determine both U/B and L. We measured[5] the orientation of the major axis of the polarization ellipse as a function of wavelength for 20 different CO_2 lines in the 10R and 10P branches between 10.2 and 10.7 μm. A pronounced linear trend was seen in the wavelength-dependent data, superimposed with substrate-interference oscillations.

The slope and intercept of the linearized θ_0 vs λ curve were $\Delta\theta_0 = 11.75°$ over $10.2 < \lambda < 10.7$ μm and $\theta_0 = 30.94°$ at $\lambda = 10.7$ μm. From this data we determined an intersection point in (U/B, L) coordinates that satisfied both θ_0 and $\Delta\theta_0$ simultaneously: U/B = –0.75 and L = 7.94 μm.

5. INTERPRETATION AND CONCLUSIONS

What did we learn about IR antennas from these measurements? The value of L = 7.94 μm is somewhat less than the "physical" length of the arm, indicating the presence of a distributed-reflection mechanism, or perhaps a reactive component to the arm-termination impedance (phase change on reflection $\neq \pi$). Phase change on reflection and armlength are essentially equivalent quantities in our model. Reflections at the ends of the arms were seen to affect the observed antenna polarization behavior, at least when the product of attenuation and arm length is ≈ 1 ($0.15\ \mu m^{-1} \times 8\ \mu m = 1.2$ for this case).

The value of U/B = -0.75 indicates that a significant unbalanced mode exists on the antenna, in addition to the balanced mode. This origin of this imbalance is probably that the MOM-diode impedance is not a pure resistance, enforcing an inter-arm phase difference at the feed that is $\neq \pi$.

6. ACKNOWLEDGMENTS

The author would like to acknowledge the contributions to this work of C. Fumeaux, W. Herrmann, and F. K. Kneubühl of the Infrared Physics Laboratory at the Swiss Federal Institute of Technology (ETH), Zürich, Switzerland, and those of H. Rothuizen of IBM Research Laboratory of Rüschlikon, Switzerland.

7. REFERENCES

1. E. Grossman, J. Sauvageau, and D. McDonald, "Lithographic spiral antennas at short wavelengths," Appl. Phys. Lett. **59**, 3225-3227 (1991).
2. I. Wilke, Y. Oppliger, W. Herrmann, and F.K. Kneubühl, "Nanometer thin-film Ni-NiO-Ni diodes for 30 THz radiation," *Appl. Phys. A* **58**, 329-341 (1994).
3. I. Wilke, W. Herrmann, and F.K. Kneubühl, "Integrated nanostrip dipole antennas for coherent 30 THz radiation," *Appl. Phys. B* **58**, 87-95 (1994).
4. C. Fumeaux, W. Herrmann, H. Rothuizen, P. DeNatale, and F.K. Kneubühl, "Mixing of 30 THz laser radiation with nanometer thin-film Ni-NiO-Ni diodes and integrated bow-tie antennas," *Appl. Phys. B* **63**, 135-140 (1996).
5. C. Fumeaux, G. Boreman, W. Herrmann, H. Rothuizen, and F.K. Kneubühl, "Polarization response of asymmetric-spiral infrared antennas," *Appl. Opt.* **36**, 6485-6490 (1997).
6. D. Rutledge, D. Neikirk, and D. Kasilingham, "Integrated-circuit antennas," in *Infrared and Millimeter Waves* **10**, K. J. Button, Ed., New York, Academic, 1983, pp. 1-90.
7. C. Brewitt-Taylor, D. Gunton, and H. Rees, "Planar antennas on a dielectric surface," Elect. Lett. **17**, 729-731 (1981).